Springer

KSME

Journal of Mechanical Science and Technology 24 (5) (2010) 1091~1096
www.springerlink.com/content/1738-494x
DOI 10.1007/s12206-010-0307-6

Three-dimensional model of spray forming by fringe element reconstruction method †

Du-Soon Choi*

Department of Machine Design, Inha Technical College, Incheon 402-752, Korea

(Manuscript Received October 26, 2009; Revised January 28, 2010; Accepted January 29, 2010)

Abstract

A three-dimensional spray forming process model was developed to predict the general transient shape of deposited material. The distribution of the spatial droplet flow rate was modeled by an axisymmetrical Gaussian function, and the shadowing effect was utilized for accurate prediction of the deposited shape. In order to construct the three-dimensional meshes applicable to various numerical analyses, the fringe element reconstruction method was employed to calculate the shape of deposited material. In order to verify the developed method, the simulation results were compared with the available experimental data in the literature. Good agreement was obtained between the numerical and experimental results. Finally, the effect of the withdrawal velocity of the substrate was investigated.

Keywords: Spray forming; Numerical analysis; Fringe element reconstruction; Billet shape; Shadowing effect

1. Introduction

Spray forming is a manufacturing process in which a bulk molten metal is converted to a spray of droplets and is deposited onto a substrate to fabricate alloys of various shapes such as strips, tubes, and billets [1-3]. It offers potential benefits in comparison with conventional casting and powder metallurgy (PM) processes. In the spray forming process, different deposition geometries can be produced by varying the substrate configuration and motion. This allows the multiple steps in PM - powder production, sieving, canning, degassing and consolidation - to be reduced to a single integrated process, while maintaining the microstructural characteristics of PM in near-net shapes. In the spray forming process, since droplets are formed by atomizing gas and nucleation occurs inside the individual droplets while they are propelled away from the atomizer and fly onto the substrate, a preform of fine-grain structure with essentially no macroscopic segregation can be obtained, allowing for alloy-homogenizing heat treatments to be avoided or shortened.

The spray forming process consists of two different steps, a spray step and a forming step. The spray step is similar to the gas atomization process. During the spray step, a molten liquid stream is fragmented into droplets by a gas field. During the forming step, the fragmented droplets are collected on a specially designed collector substrate.

The forming step is governed by many processing conditions, and therefore it is important to understand the effects of such conditions upon the overall spray forming process. Fig. 1 illustrates a typical spray forming process for production of a billet. The rotating substrate where spray droplets are deposited is withdrawn vertically to keep a constant distance between the gas atomizer and the preform top surface, which leads to steady-state deposition of spray droplets. The shape of a growing billet is determined by various processing conditions such as the flow rate of the alloy melt, the initial position of the atomizer, the angle of the spray axis, the withdrawal velocity of the substrate, and so on.

Mathur et al. [4] proposed a rod-forming model entailing numerical integration of the growth velocity of the rotating preform surface grid points during scanning spray forming. Kang and Chang [5] developed a theoretical model to predict the shape of the billet and studied the effects of the withdrawal velocity of the substrate and the cam profile, on the shape of the growing billet. Seok et al. [6, 7] developed a three-dimensional model to calculate the shape of the general preform and analyzed the shape of a spray-formed rod under various processing conditions. Hattel et al. [8, 9] developed an integrated model describing the atomization and deposition stages in the spray forming process, using a 2D cylindrical heat flow model to predict the shape of a billet in consideration of the sticking efficiency and the shading effect. Mi and Grant developed a numerical model [10] to simulate dynamic shape evolution for deposition, splashing, and redeposition or

† This paper was recommended for publication in revised form by Associate Editor Dae-Eun Kim
*Corresponding author. Tel.: +82 32 870 2153, Fax.: +82 42 870 2502
E-mail address: dschoi@inhatc.ac.kr

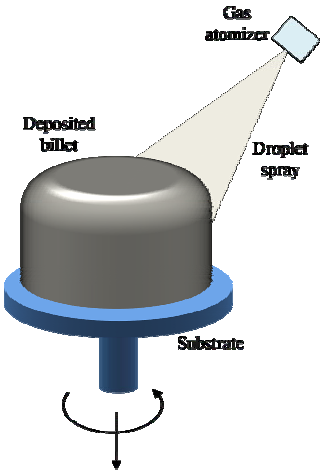

Fig. 1. Schematic diagram of spray forming process.

droplets, as well as a 2D numerical model [11] to simulate heat flow and solidification of Ni superalloy rings during spray forming.

In order to predict the shape of a billet according to processing conditions, the proposed techniques thus far have used two- or three-dimensional approaches. However, they are limited to two-dimensional approaches for numerical analyses of physical phenomena such as heat flow and solidification. For three-dimensional analysis, it is essential to construct three-dimensional meshes that fit the transient shape of the deposited material in the spray forming process.

In the present study, a three-dimensional model of a spray forming process was developed that can predict the general shape of the preform in consideration of the shadowing effect. In order to construct the three-dimensional meshes applicable to the various numerical analyses employed, the fringe element reconstruction method [12] was utilized to calculate the preform shape.

2. Numerical model

2.1 Deposition rate model

The distribution function of the spatial droplet flow rate, $\dot{M}$ (mm^3/mm^2·s), can be assumed as an axisymmetrical Gaussian function: [6]

$$\dot{M}(r) = a \cdot \exp\left(-b \cdot r^2\right). \tag{1}$$

The term $\dot{M}$ can be experimentally measured from the surface profile of the preform spray formed on a stationary substrate per unit time; r is the shortest distance from a point to the spray axis line of the distribution function. Parameters a (mm/s) and b (mm^{-2}) are the spray distribution parameters, which are dependent on the total droplet flow rate, the design of the atomizer, and the spray distance. The spray distance of a point is defined as the distance between the atomizer and the nearest point on the spray axis. The total droplet flow rate, $\overline{M}$ (mm^3/s), can be obtained by integrating $\dot{M}$ as follows:

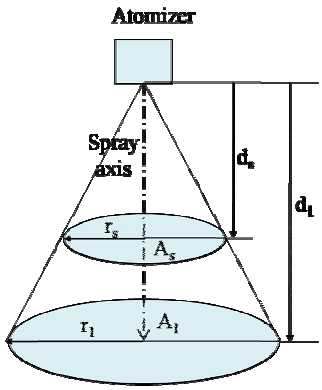

Fig. 2. Schematic diagram of droplet deposition.

$$\overline{M} = \int_0^{\infty}\int_0^{2\pi} a \cdot \exp\left(-b \cdot r^2\right) \cdot r\,d\theta\,dr = \frac{\pi a}{b}. \tag{2}$$

Fig. 2 shows a schematic diagram of droplet depositions for the spray distances of d_s and d_1. The droplet flux through the circular areas A_s and A_1 at the spray distances of d_s and d_1 should be the same. The droplet flux J_s and J_1 through the circular areas A_s and A_1, respectively, can be defined as Eq. (3). The terms r_s and r_1 are the radii of the circular areas A_s and A_1, respectively.

$$\begin{aligned} J_s &= \int_0^{r_s}\int_0^{2\pi} a \cdot \exp\left(-b \cdot r^2\right) \cdot r\,d\theta\,dr, \\ J_1 &= \int_0^{r_1}\int_0^{2\pi} a \cdot \exp\left(-b \cdot r^2\right) \cdot r\,d\theta\,dr. \end{aligned} \tag{3}$$

The geometric relation of d_s / d_1 = r_s / r_1 and volume conservation of $J_s = J_1$ yield the following relation:

$$\frac{a_s}{a_1} = \frac{b_s}{b_1} = \left(\frac{d_s}{d_1}\right)^2. \tag{4}$$

The spray distribution parameters a_s and b_s can be measured at the reference spray distance d_s. Using Eq. (4), the droplet flow rate $\dot{M}$ can be defined for any spray distance d as follows:

$$\dot{M}(a,b,r,d) = a\left(\frac{d_s}{d}\right)^2 \cdot \exp\left[-b\left(\frac{d_s}{d}\right)^2 \cdot r^2\right]. \tag{5}$$

2.2 Billet shape model

Fig. 3 shows a geometrical spray forming configuration. The droplet flow rate on a point p can be calculated by Eq. (5), where r is the shortest distance from point p to the spray axis, and d is the spray distance which can be calculated as follows:

$$d = \mathbf{e_s} \cdot (\mathbf{P} - \mathbf{A}), \tag{6}$$

where $\mathbf{P}$ is the position vector of point p, $\mathbf{A}$ is the position vector of the atomizer, and $\mathbf{e_S}$ is the unit vector of the spray

axis.

The distance r can be obtained from the vector relation as follows:

$$r = \left|\mathbf{A} + d\mathbf{e}_s - \mathbf{P}\right|. \tag{7}$$

The growth distance, Δh, of point p during a time interval, δt, along the surface normal direction of $\mathbf{e}_n$ can be given as follows: [6]

$$\Delta h = \int_t^{t+\delta t} \zeta(x,y,z,t)\dot{M}(a,b,r,d)\mathbf{e}_n \cdot \mathbf{e}_f dt\,, \tag{8}$$

where $\mathbf{e}_f$ is the unit normal vector along the line between point p and the atomizer, and ζ is the function to take into account the shadowing effect, which indicates whether point p is shaded or not. ζ is zero when shading has occurred, otherwise it is unity. The shadowing effect will be discussed further in the following sub-section.

The new position vector **P'** at time t+δt can be found as follows:

$$\mathbf{P}' = \mathbf{P} + \Delta h\mathbf{e}_n\,. \tag{9}$$

2.3 Shadowing effect

Fig. 4 shows a schematic diagram of a shadowing region. Because the billet is continuously rotating, some region of the deposition surface can be in the shade. In order to accurately predict the shape of the billet, the effect of shading has to be incorporated into the model [8].

In the fringe element reconstruction method, the deposition surface is represented by triangular elements. In each time step, each node on the deposition surface should be checked to determine whether it is shaded or not.

From each point on the deposition surface, a line is drawn from the point under consideration to the position of the atomizer, as shown in Fig. 5. If there exist some intersecting points between the line drawn from the node to the atomizer and the deposition surface triangles, this node is shaded and ζ is 0. If there is no intersection point, the node is not shaded and ζ is 1. The obtained ζ value can be used in Eq. (8) to calculate the deposition surface profile.

2.4 Fringe element reconstruction method

The calculation region for numerical analyses keeps changing its shape as time continues, due to the advancement of the deposition surface. The deposition surface generally does not coincide with its elements in an Eulerian description. To overcome this drawback, a local and temporary mesh-fitting scheme was applied by dividing elements on the deposition surface into several elements [12]. This method includes several steps, as shown in Fig. 6. Since the details for three dimensional applications are described in [12], simply the highlights of the scheme are summarized below.

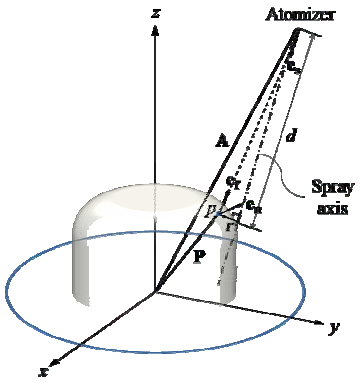

Fig. 3. Geometrical configuration of substrate, billet, and atomizer.

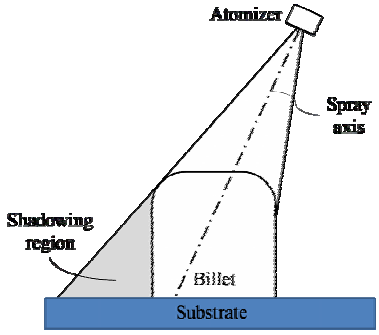

Fig. 4. Schematic diagram of shadowing region.

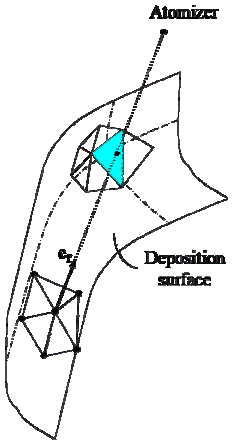

Fig. 5. Schematic diagram of intersecting point between line drawn from each point on deposition surface to atomizer and surface triangle.

2.4.1 Tracing deposition surface

Initially, the deposition surface is prescribed with triangular elements. Then, the surface can be constructed, in the next time step, by advecting the points on it according to Eq. (9).

2.4.2 Determining intersection points.

To reconstruct the fringe elements, the precise position of the intersection between the deposition surface and the element edges must be determined. In each time step, each node has a flag that indicates whether it is inside the calculation

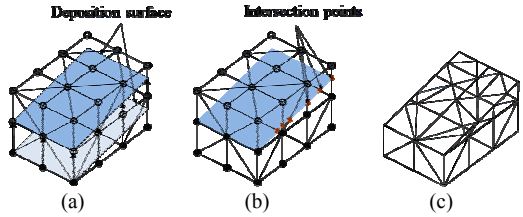

Fig. 6. Schematic diagram of fringe element reconstruction method. (a) Tracing deposit surface, (b) determining intersection points, and (c) reconstructing fringe elements.

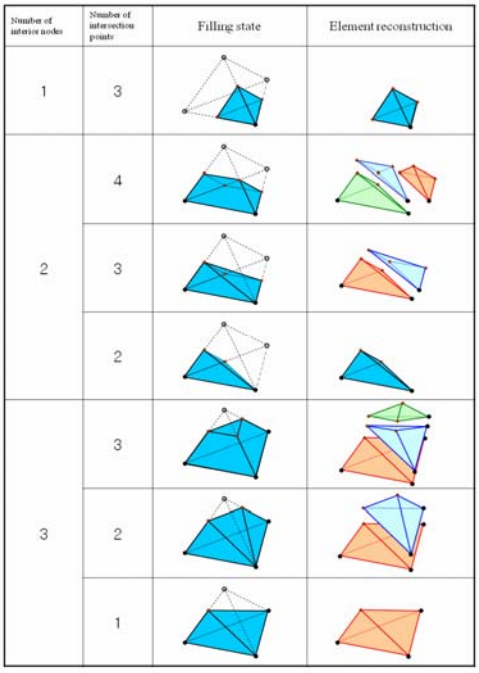

Fig. 7. Seven cases of mesh reconstruction of fringe elements.

domain or not. The nodes having flags of 1 or 0 are defined as inside or outside the calculation region, respectively. If all nodes of an element have flags of 1, it is assumed to be filled with material. If all nodes have flags of 0, the element is defined as empty. The deposition surface is located within elements that are composed of nodes that have both unity and zero flags. When the deposition surface penetrates the original mesh system, the intersection points between the surface and the element edges become new nodes for the fringe elements. Because the intersection points exist on the edges that have different nodal flags, 0 and 1, the position of the deposition surface can be roughly known. The precise position of the intersection can then be determined by finding the intersection points between those edges and the triangular elements that construct the deposition surface.

2.4.3 Reconstructing fringe elements.

Each element in which the deposition surface exists was reconstructed into several tetrahedral elements according to its filling state. Fig. 7 shows seven types of fringe elements reconstructed into an original element.

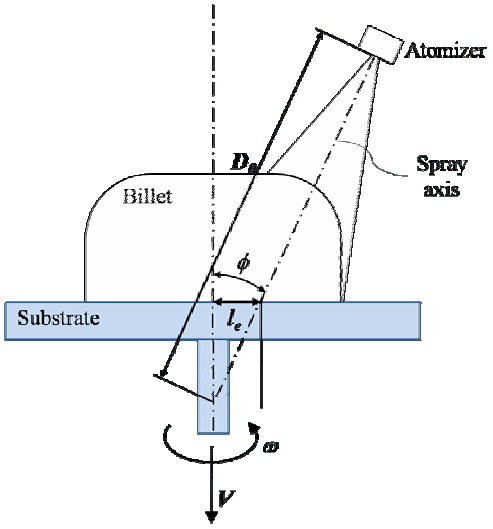

Fig. 8. Schematic diagram denoting various parameters used in numerical analysis of spray forming.

3. Results and discussion

3.1 Comparison of numerical results and experimental data

Fig. 8 shows a schematic diagram denoting various parameters used in numerical analysis of spray forming. ϕ is the angle between the rotating axis and the spray axis, D_0 is the distance between the atomizer and the intersection point of the rotation axis and the spray axis, l_e is the initial eccentric distance, ω is the rotational velocity, and V is the withdrawal velocity of the substrate.

Numerical analysis of the spray forming was performed using the currently developed numerical model. Fig. 9 shows the mesh layout employed, which contains 4834 nodes and 24285 tetrahedral elements. The processing conditions were ϕ = 35 deg, D_0 = 500 mm, l_e = 50 mm, ω = 700 deg/s, and V = 0.5 mm/s. The spray distribution parameters a_s and b_s were 2 mm/s and 0.0008 mm^{-2}, respectively. These processing conditions and parameters were chosen in order to compare the numerical results with the experimental data obtained by Seok et al. [6] as shown in Fig. 10.

Fig. 11 shows the calculated billet shapes and corresponding reconstructed mesh structures. It can be seen that the elements constituting the deposition surface exists were reconstructed into several tetrahedral elements. The geometry of the reconstructed mesh structure shows the shape of the deposited material.

Fig. 12 compares the numerical and experimental profiles for the Fig. 10 measurements. The profile of the top surface of the billet was nearly flat at the center region and convex at the edge region. The calculated profile showed good agreement with the experimental results. The measured and calculated billet diameters at the height of 150 mm were 130 mm and 132 mm, respectively. From these results, it can be confirmed that the numerical model currently developed can reasonably predict the shape and dimensions of spray-formed products.

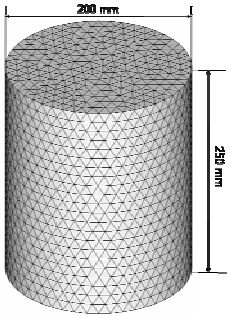

Fig. 9. Mesh layout used for numerical analysis.

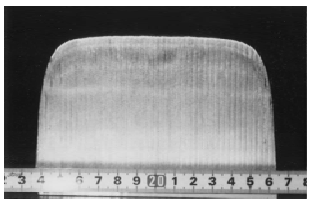

Fig. 10. Top surface profile of billet formed under processing conditions ϕ = 35 deg, D0 = 500 mm, le = 50 mm, ω = 700 deg/s, V = 0.5 mm/s, as = 2 mm/s, and bs = 0.0008 mm-2 [6].

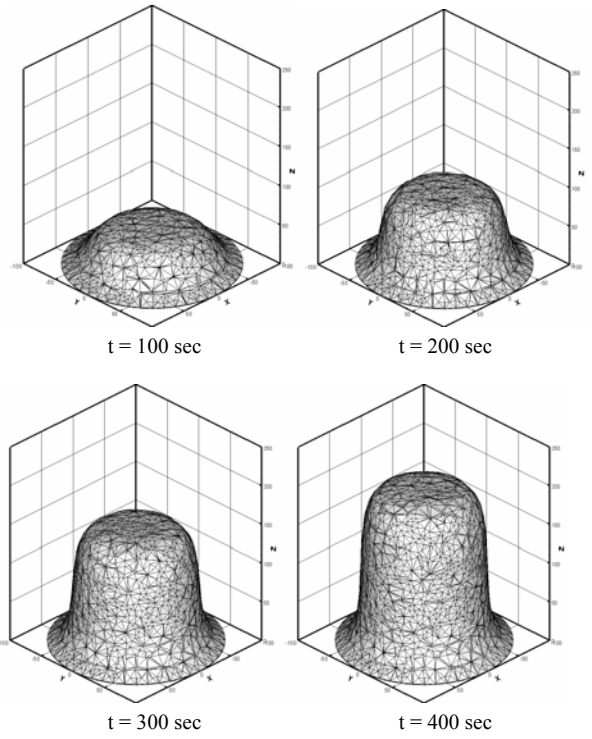

Fig. 11. Calculated billet shapes and corresponding mesh structures.

3.2 Effect of withdrawal velocity of substrate

The withdrawal velocity of the substrate is one of the most important parameters affecting the shape of the deposited material. Numerical analyses for different withdrawal velocities were performed to observe the effect of withdrawal velocity on the billet shape. Billet shapes were calculated using the same processing conditions, ϕ = 35 deg, D_0 = 500 mm, l_e = 50 mm, and ω = 700 deg/s, excepting the withdrawal velocity, which was changed to 0.25 mm/s, 0.5 mm/s, and 1.0 mm/s. The corresponding billet shapes are shown in Fig. 13.

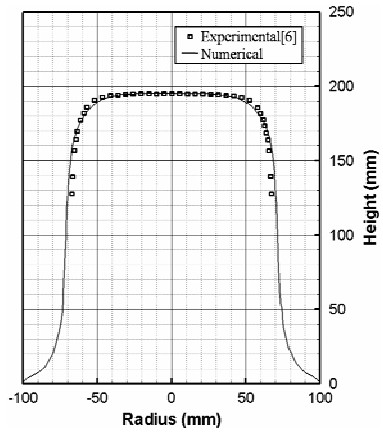

Fig. 12. Comparison of numerical and experimental surface profiles [6].

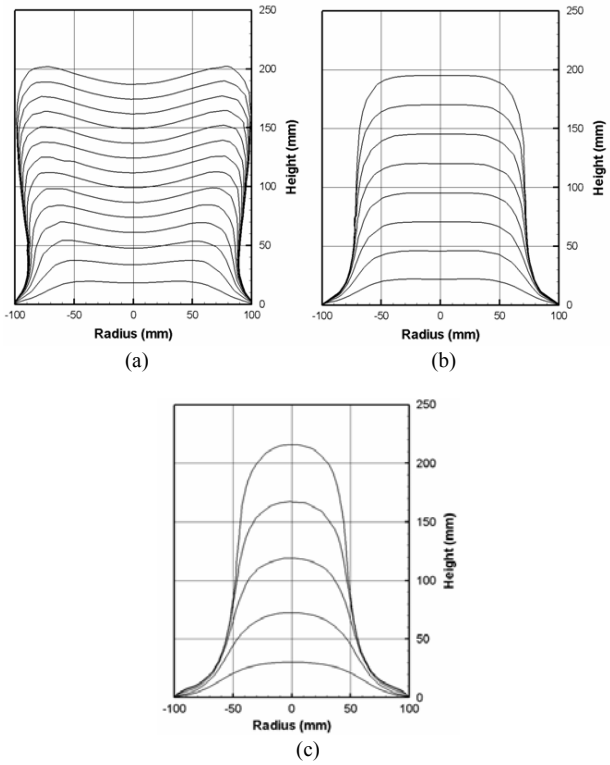

Fig. 13. Calculated shape profiles every 50 sec with various withdrawal velocities V: (a) V = 0.25 mm/s, (b) V = 0.5 mm/s, and (c) V = 1.0 mm/s.

As the withdrawal velocity V increases, the vertical growth rate of the billet increases and the diameter decreases. In the case of slow withdrawal velocity, the profile of the top surface becomes concave and the billet diameter becomes larger, because the spray axis tends towards the edge of the deposition surface, as shown in Fig. 14. In contrast, if the withdrawal velocity is fast, the billet diameter gets smaller and the profile of the top surface becomes convex, as can be seen in Fig.

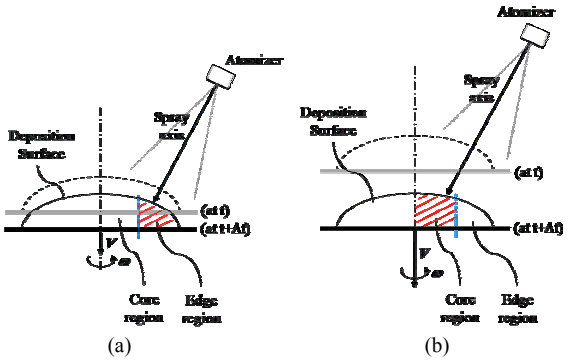

Fig. 14. Schematic diagram of intersecting points between spray axis and deposition surface in cases of (a) slow withdrawal velocity and (b) fast withdrawal velocity.

13(c).

From these results, it can be confirmed that the numerical model currently developed can reasonably analyze the transient billet shape in the spray forming process and can successfully reconstruct elements according to the shape of the billet.

4. Conclusions

A three-dimensional spray forming model that can predict the general transient shape of deposited material under various spray forming conditions in consideration of the shadowing effect, was developed. Preparatory to constructing the three-dimensional meshes applicable to the various numerical analyses, the fringe element reconstruction method was employed to calculate the shape of deposited material.

The accuracy of the developed model was verified by comparing the results to the experimental data in the literature. Also, numerical analyses for different withdrawal velocities were performed to observe the effect of withdrawal velocity on the billet shape. It was found that the model indeed was effective in three-dimensional analysis of the spray forming process.

Acknowledgment

This work was supported by Inha Technical College Research Grant.

References

[1] E. J. Lavernia and Y. Wu, *Spray Atomization and Deposition,* Wiley, New York, (1996).

[2] P. S. Grant, Spray forming, *Progress in Materials Science*, 39 (1995) 497-545.

[3] S. Annavarapu, D. Apelian and A. Lawley, Spray casting of steel strip: process analysis, *Metallurgical Transaction A,* 21A (1990) 3237-3256.

[4] P. Mathur, S. Annavarapu, D. Apelian and A. Lawley, Spray casting: an integral model for process understanding and control, *Materials Science and Engineering A*, 142 (1991) 261-276.

[5] S. Kang and D. H. Chang, Modeling of billet shapes in spray forming using a scanning atomizer, *Materials Science and Engineering A,* 260 (1999) 161-169.

[6] H. K. Seok, D. H. Yeo, K. H. Oh and H. I. Lee, A three-dimensional model of the spray forming method, *Metallurgical and Materials Transactions B*, 29B (1998) 699-708.

[7] H. K. Seok, H. C. Lee, K. H. Oh, J. C. Lee, H. I. Lee and H. Y. Ra, Formulation of rod-forming models and their application in spray forming, *Metallurgical and Materials Transactions A*, 31A (2000) 1479-1488.

[8] J. H. Hattel, N. H. Pryds and T. B. Pedersen, An integrated numerical model for the prediction of Gaussian and billet shapes, *Materials Science and Engineering A*, 383 (2004) 184-189.

[9] N. H. Pryds, J. H. Hattel, T. B. Pedersen and J. Thorborg, An integrated numerical model of the spray forming process, *Acta Materialia*, 50 (2002) 4075-4091.

[10] J. Mi and P. S. Grant, Modelling the shape and thermal dynamics of Ni superalloy rings during spray forming part 1: shape modeling – droplet deposition, splashing and redeposition, *Acta Materialia*, 56 (2008) 1597-1608.

[11] J. Mi and P. S. Grant, Modelling the shape and thermal dynamics of Ni superalloy rings during spray forming part 2: thermal modeling – Heat flow and solidification, *Acta Materialia*, 56 (2008) 1588-1596.

[12] D. S. Choi, S. S. Lee and Y. T. Im, Fringe element reconstruction for front tracking for three-dimensional incompressible flow analysis, *International journal for numerical methods in fluids*, 48 (2005) 631-648.

Du-Soon Choi received his B.S. degree in Mechanical Engineering from KAIST, in 1997. He was awarded his M.S. and Ph.D degrees from KAIST in 1999 and 2005, respectively. Dr. Choi is currently a Professor at the Dept. of Machine Design at Inha Technical College in Incheon, Korea. His research interests include numerical analysis and injection molding.